Hindawi Publishing Corporation
Journal of Chemistry
Volume 2015, Article ID 370906, 10 pages
http://dx.doi.org/10.1155/2015/370906

Research Article

Effect of PAN Oxidation on the Electrochemical Lithium Insertion/Deinsertion Behavior of Resultant Carbons

Aleksandra Piotrowska, Krzysztof Kierzek, and Jacek Machnikowski

Division of Polymer and Carbonaceous Materials, Faculty of Chemistry, Wrocław University of Technology, Wybrzeże Wyspiańskiego 27, 50-370 Wrocław, Poland

Correspondence should be addressed to Jacek Machnikowski; jacek.machnikowski@pwr.edu.pl

Received 1 December 2014; Accepted 16 February 2015

Academic Editor: Cecile Autret-Lambert

The effect of polyacrylonitrile (PAN) oxidation on the properties and electrochemical lithium insertion/deinsertion behavior of carbons produced in the temperature range of 1000–1150°C has been assessed. Air-treatment at 220 and 240°C modifies essentially the carbonization behavior of polymer leading to materials with developed microporosity and enhanced oxygen content in contrast to practically nonporous pristine PAN-based carbon. The extent of the modification increases with the oxidation depth and decreases with HTT. Galvanostatic charge/discharge reveals typical hard carbons characteristics of all the materials. PAN-based carbon heat-treated at 1050°C represents most promising anodic performance. It gives reversible capacity (C_{rev}) near 420 mAh g^{-1} with a reasonable coulombic efficiency during cycling of ~99% and a moderate low voltage capacity of 100 mAh g^{-1}. Extensive oxidation enhances overall 1st discharge cycle capacity to 870 mAh g^{-1} and C_{rev} to 560 mAh g^{-1}; however, large irreversible capacity (C_{irr}) and poor cycleability are serious drawbacks of all carbons from oxidized PAN. Pyrolytic carbon coating using methane CVD at 830°C is effective in suppressing C_{irr} by about 30% but the cycleability remains nonacceptable.

1. Introduction

Nongraphitizable "hard" carbons produced by the heat-treatment of some polymer precursors at about 1000°C have been widely studied in the past as a potential anode material of lithium-ion battery [1–8]. The hopes have arisen from the enhanced, compared to graphite, capacity for lithium storing. However, excessive irreversible trapping of lithium during the first discharging cycle, large hysteresis in the voltage profile, and a considerable part of insertion occurring at the potential near 0 V versus Li/Li$^+$ cause hard carbons to be considered as inferior to graphite for most common applications in the mobile electronics sector. Recent interest in the development of medium and large scale batteries for new fields of applications, especially pure and hybrid electric vehicles [9, 10], revived the interest in hard carbons. The inexpensive precursor and a facile synthesis route are in favor of using this type of anode material.

In general, the characteristic behavior of hard carbons during charging and discharging is related to the disordered structure of the materials and associated porosity. EPR analysis shows that during discharging lithium first intercalates carbon crystallites and later fills in micropores [11]. Removing lithium on charging follows the same sequence. The voltage hysteresis is attributed to the interactions between lithium and disordered matter surrounding micropores. ^{7}Li NMR study reveals a few types of lithium bonding with the host lattice, corresponding to interactions with graphene layers, different type of active sites associated with the edges, structural defects, and heteroatoms as well as filling microcavities with pseudo-metallic lithium clusters [9, 12–14]. The sites available to lithium accommodation during the first discharge cycle vary in number and quality dependening on the carbon composition, structure, and texture.

Polyacrylonitrile (PAN) belongs to polymers of great importance for the technology of carbon materials due to widespread use for carbon fiber manufacturing. PAN-based carbons, including particulates [15, 16], microspheres [17], fibers [18], and nanofibers [19] have received also some attention as anode material of Li-ion cell. Nitrogen substituted

for carbon in the ring, that is, the characteristic feature of PAN-based carbons, may contribute to trapping lithium, thus contributing to enhanced irreversible capacity [16]. On the other hand, vacancies left after the nitrogen evolution on heat-treatment are considered as new sites for lithium insertion [20]. Recently, it has been demonstrated [17] that elevating the heat-treatment temperature (HTT) of PAN-based carbons above 1000°C can lead to the considerable decrease in irreversible capacity with a limited loss of reversible capacity [17].

Recently, we have assessed the potential of carbons prepared at 1000°C from several common polymers for the electrochemical lithium storage [21]. The comparative study showed that there was no straight correlation between the lithium uptake during the first discharge cycle and microporosity development. The PAN-based carbon was amongst materials with the highest uptake despite the fact that it was practically nonporous. Though a large part of the lithium was trapped irreversibly, the reversible capacity was still quite attractive, about 370 mAh g^{-1}.

Mild oxidation in air of as-spun fibers, called stabilization, is a common pretreatment step in manufacturing PAN-based carbon fibers [22]. Oxygen-induced dehydrogenation, cyclization, and aromatization reactions modify essentially the behavior of polymer on heat-treatment and the properties of resultant carbons. In the present work we try to assess the effect of PAN oxidative pretreatment and carbonization temperature on the lithium insertion/deinsertion properties of resultant carbons in relation to their chemical composition, structural ordering, and porosity. In previous studies concerning PAN-based carbons as anode material this aspect has not received any special attention. Coating with pyrolytic carbon (PC) has been applied for deactivating active sites, thus decreasing the irreversible capacity [4, 23, 24].

2. Experimental

2.1. Preparation of PAN-Based Carbons. Polyacrylonitrile (PAN) powder from Aldrich (particle size < 0.3 mm) was used as starting material. Oxidized forms of the polymer were prepared by the treatment in air at 220°C (PAN22) and 240°C (PAN24) for 4 h. Carbonization was performed in a horizontal tube furnace by heating under nitrogen to 1000, 1050, 1100, and 1150°C at a rate of 5 K/min, followed by soaking for 2 h. The resultant carbons PAN-100, PAN22-100, PAN24-100, PAN-105, and so forth were ground to the particle size of <63 μm. For coating with pyrolytic carbon (CVD), the powders, placed in a quartz boat, were heated in the mixture of 10 vol% of methane in nitrogen at 830°C for 0.75 h (PAN-100) or 1.5 h (PAN22-100 and PAN24-100) to fill in the accessible porosity. The symbols of coated carbons were created by adding "d" (e.g., PAN-100d).

2.2. Structural and Textural Characterization. The carbons were characterized in terms of chemical composition, structural arrangement (XRD), and microporosity development.

CHNS contents were determined using the elemental analyzer CHNS VARIO EL (Elementar Analysensysteme GmbH). The oxygen content was measured directly on the Carlo Erba analyzer.

X-ray diffraction measurements were performed on Rigaku powder diffractometer ULTIMA IV using $Cu_{k\alpha}$ radiation (λ = 0.15406 nm) and 40 kV accelerating voltage. The structural parameters calculated from the XRD spectra included the interlayer distance d_{002} and crystallite height L_c and diameter L_a. L_c and L_a values were calculated from the width at the half maximum of 002 and 10 bands, respectively, using the Scherrer equation [25].

The porous texture was characterized by the adsorption of nitrogen at 77 K (ASAP2020, Micromeritics) and carbon dioxide at 273 K (NOVA 2200, Quantachrome). Before measuring the samples were degassed overnight at 300°C. N_2 adsorption isotherms were used to determine the total pore volume V_T, BET surface area S_{BET}, and microporosity (<2 nm width) development. Micropore volumes V_{DR} and mean size L_0 were calculated using the Dubinin-Radushkevich [26] and Stoeckli [27] equations to adsorption data up to relative pressure of $p/p_0 < 0.08$. The QSDFT analysis [28] was applied to N_2 adsorption isotherms obtained using ASAP 2020 to determine pore size distribution (PSD) and micropore surface area (S_{QSDFT}).

The CO_2 adsorption isotherms at low pressure < 10 kPa are assumed to correspond to the adsorption in ultramicropores, narrow micropores of size < 0.7 nm. They were used for the calculation of the ultramicropore volume V_{DRCO_2}. The DFT method was applied to the CO_2 adsorption isotherms to determine the ultramicropore size distribution.

2.3. Electrochemical Measurements. Electrochemical tests were performed in a coin-type cell (CR2032, Hohsen Corp., Japan), which was assembled with carbon electrode as an anode and metallic lithium foil as a cathode and reference electrode. Electrolyte used was 1 M solution of lithium hexafluorophosphate ($LiPF_6$) in a mixed solvent EC : DMC, 1 : 1 by volume. A glass microfiber separator (Whatman, GF/F, thickness of 420 μm) wetted with the electrolyte was sandwiched between the carbon electrode and Li foil. The electrodes of 6–8 mg mass, 14 mm diameter, and 100 μm thick were pressed from a mixture of active material (85%), PVDF binder (10%), and conducting carbon black (5%).

The standard test of the assembled lithium/carbon half-cell comprised discharging to 0.005 V versus Li and 25 full charge/discharge cycles between 0.005 and 1.5 V. The lithium insertion into carbon material (cell discharge) was performed using a constant current + constant voltage mode (CC + CV) with the current density set at $C/2 + C/100$, where C corresponds to the theoretical capacity of graphite (372 mAh/g) in 2 and 100 h, respectively. The deinsertion occurred at a current density of $C/5$. The galvanostatic characteristics of a cell were used to determine the total first discharge capacity (C_T), reversible capacity C_{rev}, and irreversible capacity C_{irr}. Coulombic efficiency CE was calculated as the ratio of deinsertion to insertion charge. In addition the capacity corresponding to the low voltage plateau, that is, below 40 mV (C_{LV}), was assessed from the second discharge cycle. All the measurements were performed using multichannel potentiostat/galvanostat VMP3 (Biologic, France).

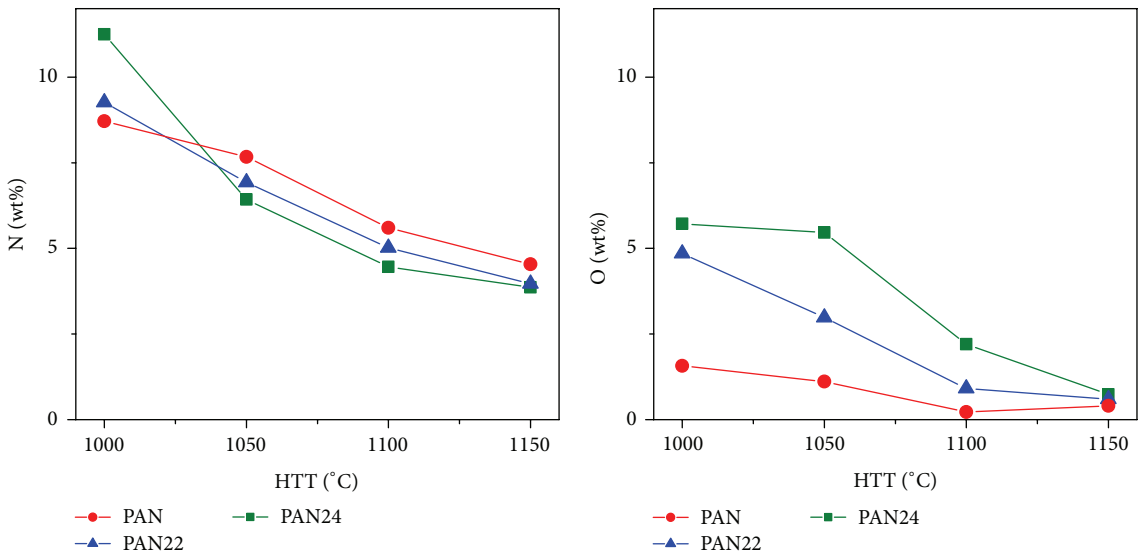

Figure 1: Effect of HTT on nitrogen and oxygen contents in PAN-based carbons.

3. Results and Discussion

3.1. Effect of PAN Oxidation on the Properties of Resultant Carbons. Elemental analysis was used to assess the extent of PAN oxidation. The data (Table 1) show that the treatment of pristine PAN in air at 220°C is reflected mostly by an increase in oxygen content. Elevating the temperature to 240°C induces considerable dehydrogenation, in addition to extensive oxygen functionalization.

Increasing HTT from 1000 to 1150°C induces a gradual heteroatom evolution from carbonaceous material (Figure 1). Oxidative pretreatment results in an enhanced oxygen content in carbons produced at 1000 and 1050°C; however, the contribution decreases steeply with HTT to about 0.5 wt% in 1150°C carbons. Nitrogen evolution is less affected by PAN oxidation and HTT; carbons heated at 1150°C still contain 4–4.5 wt% of nitrogen. All carbons are characterized by low hydrogen content, below 0.6 wt%. Corresponding H/C atomic ratio is in the range of 0.05–0.08, slightly diminishing with HTT. It proves that only residual hydrogen remains at the edges of graphene layers.

X-ray diffraction patterns of PAN-based carbons (Figure 2) are typical of poorly organized material. Polymer oxidation slightly improves structural ordering of resultant carbon. Interlayer distance d_{002} decreases from 0.358 to 0.355 nm and crystallite diameter L_a increases from 2.9 to 3.6 nm. The statistical stack contains about four defective graphene layers.

Figure 3 presents N_2 adsorption isotherms and pore size distribution of carbons from pristine and oxidized PAN produced at 1000 and 1050°C. As has already been reported [20] pristine PAN-based carbon practically does not contain pores wider than about 0.5 nm in contrast to those from oxidized PAN (Figure 3(a)). The volume and surface area of micropores accessible to nitrogen at 77 K are small and decrease with HTT (Table 2) to become negligible for carbons heated at 1100 and 1150°C.

Table 1: Elemental composition of pristine and oxidized PAN.

Sample	C [wt%]	H [wt%]	N [wt%]	O [wt%]
PAN	67.0	5.6	25.9	1.2
PAN22	64.8	5.0	24.4	5.6
PAN24	62.9	3.2	22.6	11.2

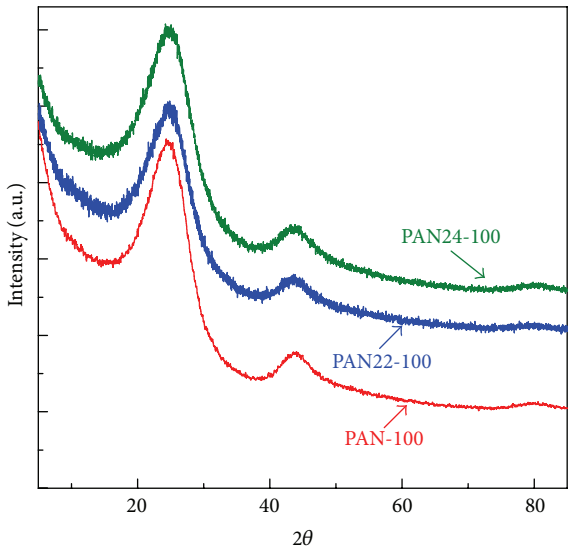

Figure 2: X-ray diffraction patterns of 1000°C carbons from pristine and oxidized PAN.

PSD calculated by applying QSDFT analysis to the isotherms (Figure 3(b)) reveals mostly very narrow micropores, of width close to 0.6 nm. A measurable amount of wider micropores appears in PAN24-100 only.

CO_2 adsorption at 273 K is used here to follow the ultramicroporosity (<0.7 nm width) development that cannot be properly analyzed by N_2 adsorption at 77 K due

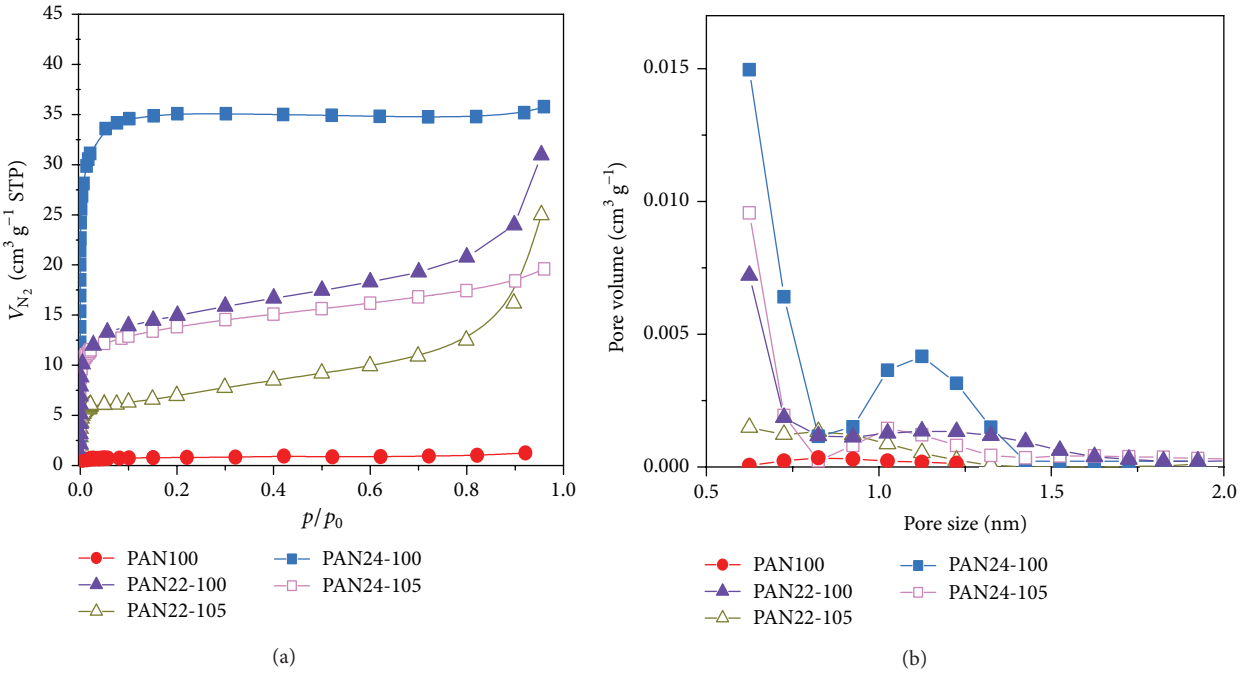

Figure 3: N_2 adsorption isotherms (a) and pore size distribution (b) of PAN-based carbons.

Table 2: Porosity parameters of PAN- PAN22- and PAN24-based carbons.

Sample	V_T [cm^{3}g^{-1}]	V_{DR} [cm^{3}g^{-1}]	S_{QSDFT} [m^{2}g^{-1}]
PAN-100	0.002	0.002	3.1
PAN22-100	0.048	0.020	58
PAN24-100	0.055	0.050	154
PAN22-105	0.039	0.019	26
PAN24-105	0.030	0.011	57

to diffusional restrictions [29]. Comparison of adsorption isotherms (Figure 4(a)) and PSD profiles (Figure 4(b)) of carbons heat-treated at 1000 and 1150°C shows very little CO_2 uptake in case PAN-based carbons that strongly increases with the polymer oxidation progress but decreases with HTT. Quantitative evaluation (Figure 5) shows 3-fold decrease in ultramicropore volume V_{DRCO_2} for PAN24-based carbons and 2-fold for PAN22-based with HTT increase from 1000 to 1150°C.

3.2. Electrochemical Measurements. Basically, voltage capacity characteristics from galvanostatic charge/discharge cycling of the polyacrylonitrile-based materials reveal all characteristic features which are specific of lithium insertion and deinsertion in hard carbons. Compared to graphite, there are distinctly higher capacity for lithium storing during the first discharge, excessive amount of irreversibly bound Li, and the enlarged charge/discharge hysteresis (Figure 6). The extent of the phenomena is markedly higher for carbons from oxidized PAN than for PAN-based. Increasing HTT from 1000 to 1150°C has a less pronounced effect on the voltage profile of carbons from a given precursor; however, some decrease in the capacities and hysteresis loop should be noticed. 1150°C from PAN (a), PAN22 (b), and PAN24 (c).

Figure 7 presents the variation in the first discharge capacity C_T, corresponding to the overall capability for lithium storing, with HTT. In general, the capacity is considerably higher than that of graphite, reaching 650 mAh g^{-1} for carbons from pristine PAN (PAN-100) and 880 mAh g^{-1} for those derived from oxidized PAN (PAN24-100). In case of carbons from pristine PAN possible sites for excessive lithium storing are heteroatoms and microcavities associated with distortion of graphene layers due to the presence of nitrogen substituted for carbon in the ring. Very little porosity of the carbons suggests that the microcavities are inaccessible for molecules of nitrogen and carbon dioxide used in sorption analysis. Relatively low H/C atomic ratio indicates that binding lithium to hydrogen atoms, the mechanism dominating for low-temperature carbons [1], has a minor contribution to the capacity. Further enhancement of C_T for carbons from oxidized PAN can be attributed mostly to lithium storing in ultramicroporosity, according to the generally accepted mechanism [1, 2]. The increase in HTT from 1000 to 1150°C results in a lower C_T by 100–150 mAh g^{-1}. Both the reduction of porosity and heteroatom content can contribute to the decrease.

The variation of the reversible capacity C_{rev}, taken here from the second discharge cycle, with HTT (Figure 8) follows the trend observed on Figure 7; however, C_{rev} values are lower by 35–40% than corresponding C_T. The gap, amounting to 190–310 mAh g^{-1}, proves that a large part of lithium is irreversibly trapped in the carbon. On the other hand, either polymer oxidation or HTT have no essential effect

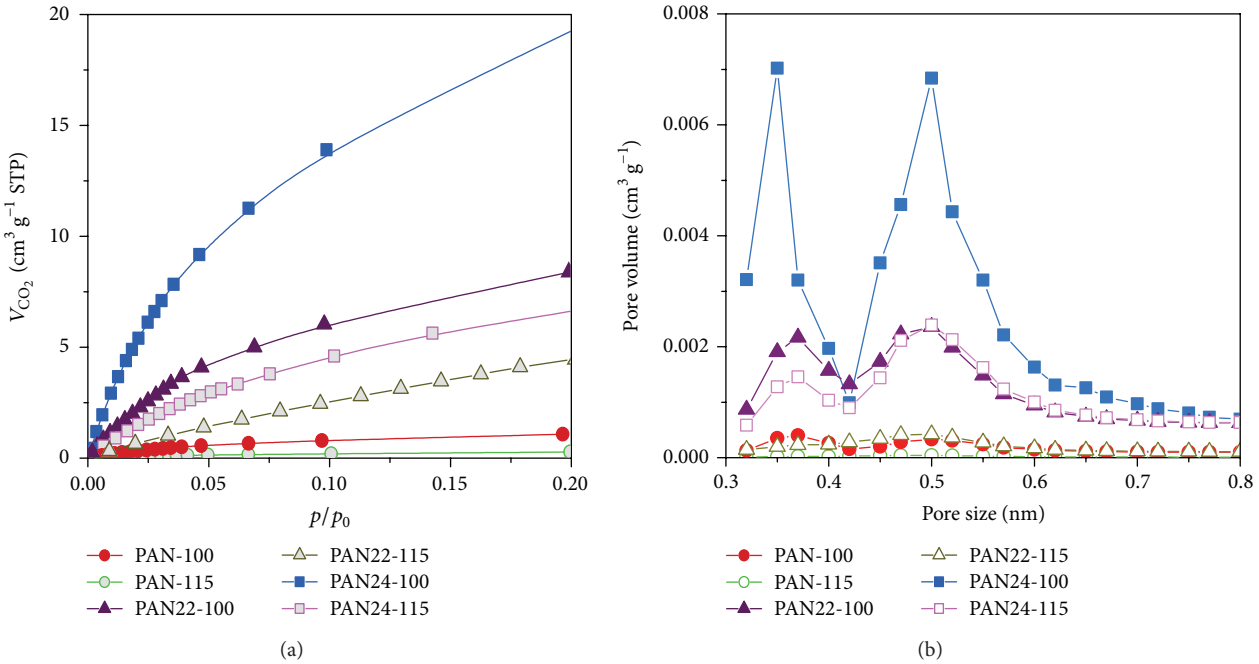

Figure 4: CO_2 adsorption isotherms of 1000°C carbons from pristine and oxidized PAN.

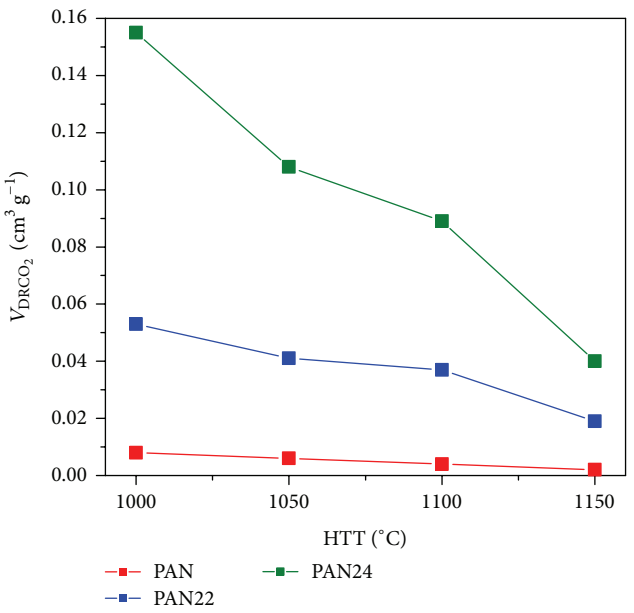

Figure 5: Effect of HTT on the ultramicropore volume V_{DRCO_2} of carbons from pristine and oxidized PAN.

on the contribution of C_{irr} to C_T. As a rule the reversible capacity increases with the extent of PAN oxidation but slightly decreases with HTT. An unexpected exception is a marked maximum of reversible capacity for PAN-based carbon heat-treated at 1050°C. The essential increase in C_{rev} compared to PAN-100 (418 versus 373 mAh g^{-1}) is a combined effect of preserving the overall capability of lithium insertion and significant reduction of irreversible capacity. So big improvement can hardly be understood keeping in mind slight differences in the chemical composition and porosity between PAN-105 and PAN-100.

The study shows that micropores wider than about 0,6 nm, which are measurable by N_2 adsorption at 77 K, are not necessary to increase the reversible capacity above 372 mAh g^{-1}. In case of PAN-based carbons, rather very narrow microcavities associated with defects in the crystallite structure are crucial for the excess in the lithium storage. The contribution from ultramicropores accessible for CO_2 molecules (>0.33 nm) seems to be meaningful for carbons from deeply oxidized polymer, especially of PAN24 series.

A large contribution of lithium insertion in the low voltage versus Li/Li$^+$ region has been considered as one of drawbacks in the use of hard carbons as anode material [10]; however, any quantitative estimation of the contribution has not been published. Figure 9 shows the effect of carbon origin and HTT on the capacity corresponding to the lithium insertion occurring in the voltage from 40 and 5 mV during the second discharge. The data clearly show a strong effect of polymer oxidation. C_{LV} is about 3 times higher for PAN22- and PAN24-based carbons compared to PAN-based ones. In case of the former carbons the low voltage capacity accounts for about 50% of the reversible capacity but in case of the latter for about 25% only. Taking into account a similarity in elemental composition and structural ordering of all carbons studied there is no doubt that this part of capacity corresponds to lithium filling ultramicropores.

The long term performance of carbons used in the study was compared in 25-cycle test of the galvanostatic charge/discharge. Figure 10(a) shows quite good capacity

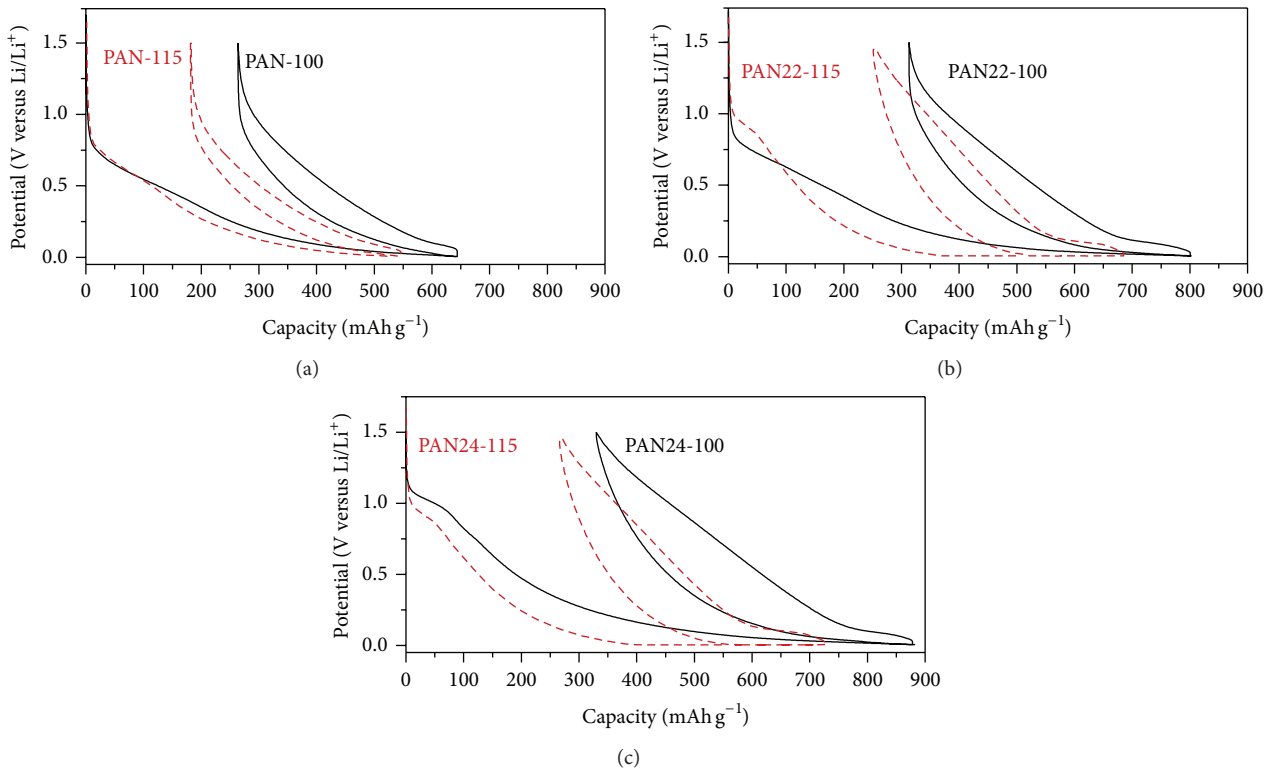

Figure 6: Galvanostatic insertion/deinsertion of lithium into hard carbons produced at 1000 and 1150°C from PAN (a), PAN22 (b), and PAN24 (c).

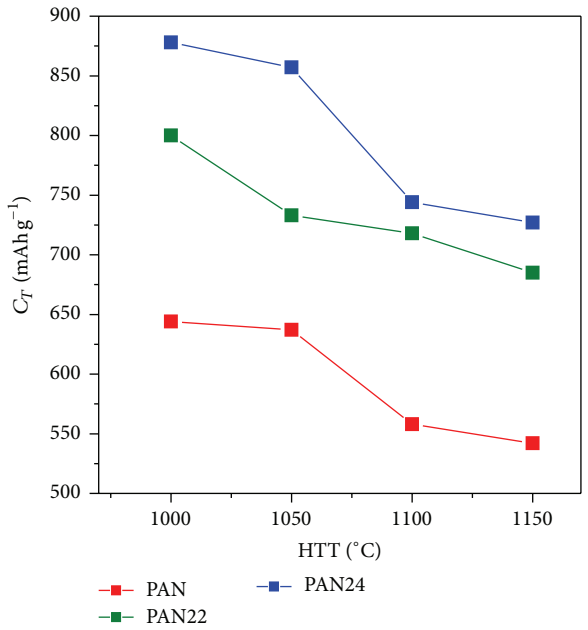

Figure 7: Variation of the first discharge lithium insertion capacity with HTT of pristine and oxidized polyacrylonitrile.

stability and high coulombic efficiency of all PAN-based carbons. The highest capacity prefers PAN-105. Cycling tests of PAN22- and PAN24-based carbons show distinct capacity fall; however the performance improves with increase in HTT. Capacity fading seems to be related to the presence of porosity in the materials. It can be considered as an effect of the gradual destruction of disordered material occurring around micropores due to interaction with lithium [11]. Drastic capacity loss is associated with a significant decrease of the coulombic efficiently, even down to 95% (Figure 10(c)).

Table 3: Porosity parameters and reversible and irreversible capacity values for the first cycle discharge charge.

Sample	V_{DRCO_2} [$cm^3 g^{-1}$]	C_{rev} [$mAhg^{-1}$]	C_{irr} [$mAhg^{-1}$]	C_T [$mAhg^{-1}$]	CE1	C_{LV} [$mAhg^{-1}$]
PAN-105	0.008	418	219	637	0.66	103
PAN-105d	0.003	432	212	644	0.67	100
PAN22-100	0.053	487	313	800	0.61	217
PAN22-100d	0.022	474	212	686	0.69	256
PAN24-100	0.155	549	329	878	0.63	231
PAN24-100d	0.030	534	252	786	0.68	261

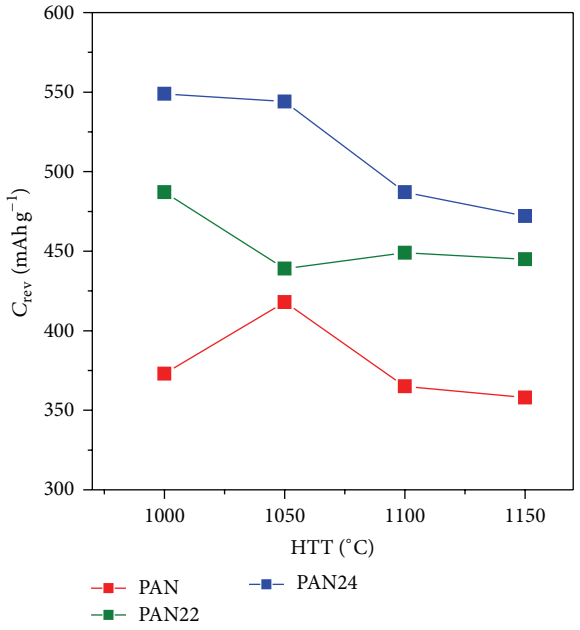

Figure 8: Variation of the reversible capacity with HTT of pristine and oxidized polyacrylonitrile.

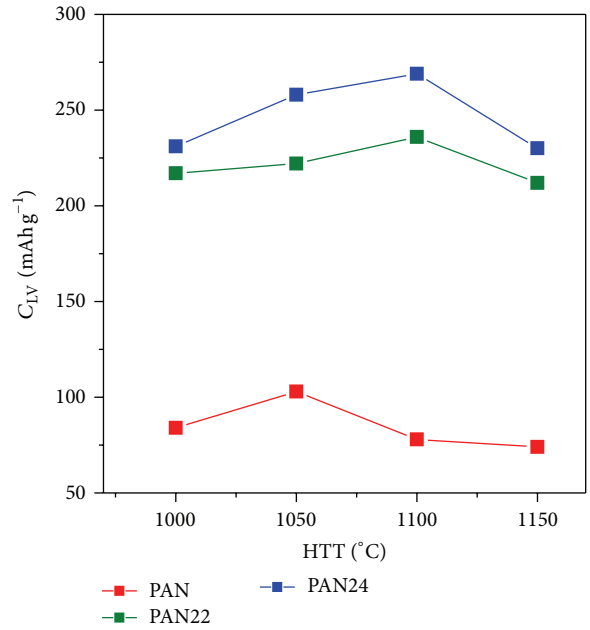

Figure 9: Variation of the low voltage reversible capacity with HTT of pristine and oxidized polyacrylonitrile.

3.3. Effect of Pyrolytic Carbon Coating on the Properties of PAN-Based Carbons. In the study coating was carried out under very mild condition to allow methane penetration inside porous system and PC deposition on pore walls. Under these conditions a partial pore filling occurs before a shell on the outer particle surface is finally formed. PAN-105, PAN22-100, and PAN24-100 as representing the highest reversible capacity amongst carbons from each precursor were selected for the treatment.

CVD appeared to be quite effective in reducing ultramicroporosity of PAN22-100 and PAN24-100. V_{DRCO_2} decreases about 2.5 and 5 times, respectively (Table 3). Voltage-capacity profiles from galvanostatic charge/discharge cycling (Figure 11) show a negligible effect of CVD on the performance of PAN-105 but quite marked reduction of irreversible capacity and charge/discharge hysteresis when the treatment is applied to PAN22-100 and PAN24-100. First cycle coulombic efficiency increases from 0.61 and 0.63 to 0.69 and 0.68, respectively, as an effect of suppressing the irreversible capacity by 80–90 mAh g^{-1} with a little change of reversible capacity (Table 3).

Although the materials porosity is distinctly decreased by increasing HTT and carbon deposition, the irreversible capacity still remains relatively high (more than 200 mAh/g). It means that only minor part of C_{irr} is related to the formation of SEI. Most lithium is trapped inside the carbon structure, on nitrogen atoms, and in closed microcavities. Carbon coating but also HTT increasing are believed to enhance the contribution of closed microcavities. They are filled in the low voltage region and can serve as reservoirs for lithium storing only during first discharging because they are not emptied during charging. The explanation is consistent with the enhancement by 30–40 mAh g^{-1} of the insertion occurring in the low voltage region (C_{LV}) in the coated carbons, despite considerably reduced V_{DRCO_2}. In consequence, any treatment applied in the study could not increase CE1 above 0.7.

The long term performance test (Figure 12) shows that PC deposition under conditions used in the study induces only slight improvement of the capacity stability compared to PAN22-100 and PAN24-100 behavior. Increasing HTT seems to be a more preferred route to improve the performance of carbons from oxidized polyacrylonitrile.

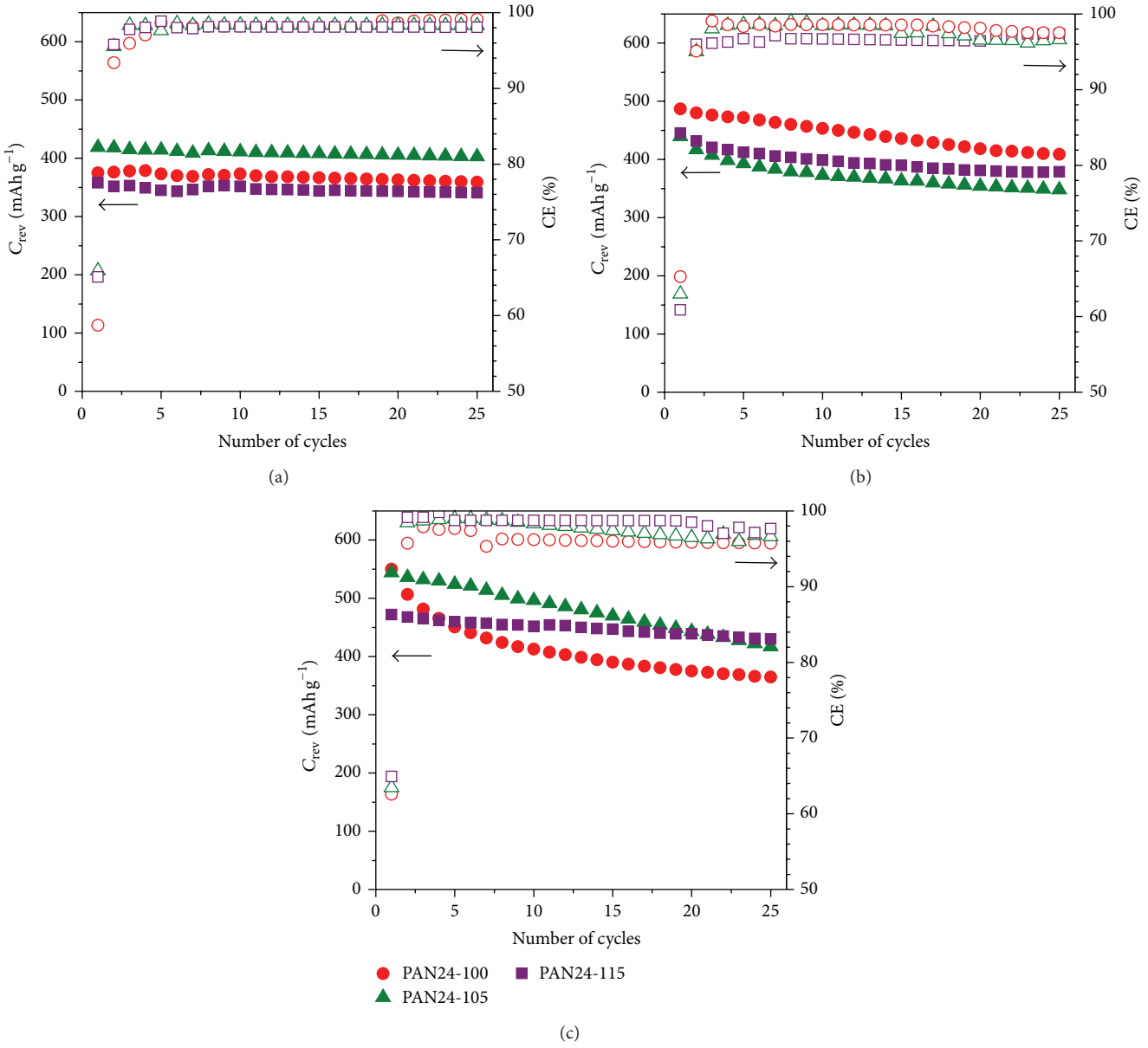

Figure 10: Cycleability of PAN-based (a), PAN22-based (b), and PAN24-based (c) carbons produced at different HTT.

4. Conclusions

Heat-treatment of polyacrylonitrile in the temperature range of 1000–1150°C gives practically nonporous hard carbons of nitrogen content decreasing with HTT from 8.7 to 5 wt%. Galvanostatic charge/discharge using constant current + constant voltage mode ($C/2 + C/100$) reveals very attractive lithium insertion capability of the carbons, corresponding to the first discharge capacity of 650 mAh g^{-1}. Heat-treatment at 1050°C is optimal for PAN-based carbons giving reversible capacity above 400 mAh g^{-1}, with a reasonable coulombic efficiency during cycling of ~99% and a moderate low voltage capacity of 100 mAh g^{-1}. Air-oxidation modifies essentially PAN behavior during the subsequent heat-treatment giving carbons with developed ultramicroporosity and the overall first discharge capacity up to 880 mAh g^{-1} and reversible capacity up to 560 mAh g^{-1}. The extent of the properties modification increases with elevating the oxidation temperature from 220 to 240°C but decreases with carbon HTT. High irreversible capacity and poor cycleability are drawbacks of carbons from oxidized PAN. Pyrolytic carbon coating using methane CVD at 830°C is effective in suppressing the irreversible capacity of the carbons by 30% with a little change of reversible capacity; however the improvement in the cycleability is nonsatisfactory.

Conflict of Interests

The authors declare that there is no conflict of interests regarding the publication of this paper.

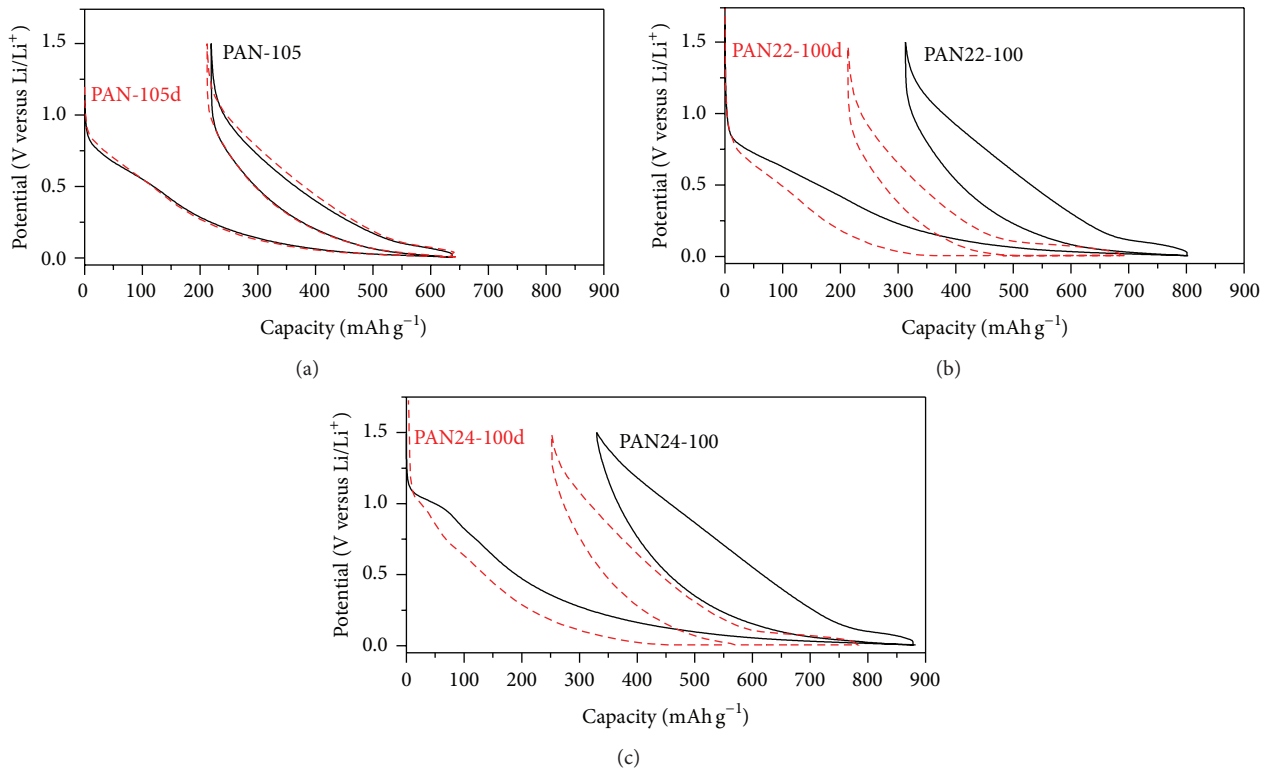

Figure 11: Effect of pyrolytic carbon coating on the galvanostatic lithium insertion/deinsertion in PAN-105 (a), PAN22-100 (b), and PAN24-100 (c).

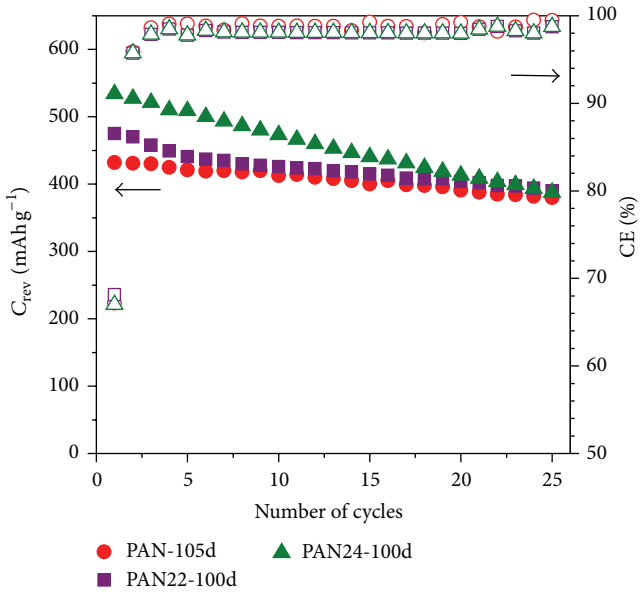

Figure 12: Cycleability of pyrolytic carbon coated PAN-105, PAN22-100, and PAN24-100.

Acknowledgment

The research was supported by Wroclaw Research Centre EIT+ within the project "The Application of Nanotechnology in Advanced Materials," NanoMat (POIG.01.01.02-02-002/08), financed by the European Regional Development Fund (Innovative Economy Operational Programme, 1.1.2).

References

[1] Y. Zheng and J. R. Dahn, "Aplications of carbon in lithium-ion batteries," in *Carbon Materials for Advanced Technologies*, T. D. Burchell, Ed., pp. 341–387, Pergamon, Amsterdam, The Netherlands, 1999.

[2] E. Buiel and J. R. Dahn, "Li-insertion in hard carbon anode materials for Li-ion batteries," *Electrochimica Acta*, vol. 45, no. 1, pp. 121–130, 1999.

[3] S. Flandrois and B. Simon, "Carbon materials for lithium-ion rechargeable batteries," *Carbon*, vol. 37, no. 2, pp. 165–180, 1999.

[4] F. Béguin, F. Chevallier, C. Vix, S. Saadallah, J. N. Rouzaud, and E. Frackowiak, "A better understanding of the irreversible lithium insertion mechanisms in disordered carbons," *Journal of Physics and Chemistry of Solids*, vol. 65, no. 2-3, pp. 211–217, 2004.

[5] H. Fujimoto, K. Tokumitsu, A. Mabuchi, N. Chinnasamy, and T. Kasuh, "The anode performance of the hard carbon for the lithium ion battery derived from the oxygen-containing aromatic precursors," *Journal of Power Sources*, vol. 195, no. 21, pp. 7452–7456, 2010.

[6] W. Li, M. Chen, and C. Wang, "Spherical hard carbon prepared from potato starch using as anode material for Li-ion batteries," *Materials Letters*, vol. 65, no. 23-24, pp. 3368–3370, 2011.

[7] J. Yang, X.-Y. Zhou, J. Li, Y.-L. Zou, and J.-J. Tang, "Study of nano-porous hard carbons as anode materials for lithium ion

batteries," *Materials Chemistry and Physics*, vol. 135, no. 2-3, pp. 445–450, 2012.

[8] L. C. Zhang, Z. Hu, L. Wang, F. Teng, Y. Yu, and C. H. Chen, "Rice paper-derived 3D-porous carbon films for lithium-ion batteries," *Electrochimica Acta*, vol. 89, pp. 310–316, 2013.

[9] K. Gotoh, M. Maeda, A. Nagai et al., "Properties of a novel hard-carbon optimized to large size Li ion secondary battery studied by ^{7}Li NMR," *Journal of Power Sources*, vol. 162, no. 2, pp. 1322–1328, 2006.

[10] P. Novák, D. Goers, and M. E. Spahr, "Carbon materials in lithium-ion batteries," in *Carbons for Electrochemical Energy Storage and Conversion Systems*, F. Beguin and E. Frackowiak, Eds., Advanced Materials and Technologies, pp. 263–328, CRC Press, New York, NY, USA, 2009.

[11] Y.-P. Wu, C.-R. Wan, C.-Y. Jiang, S.-B. Fang, and Y.-Y. Jiang, "Mechanism of lithium storage in low temperature carbon," *Carbon*, vol. 37, no. 12, pp. 1901–1908, 1999.

[12] K. Guérin, M. Ménétrier, A. Février-Bouvier, S. Flandrois, B. Simon, and P. Biensan, " ^{7}Li NMR study of a hard carbon for lithium-ion rechargeable batteries," *Solid State Ionics*, vol. 127, no. 3, pp. 187–198, 2000.

[13] M. Letellier, F. Chevallier, C. C. Clinard et al., "The first in situ ^{7}Li nuclear magnetic resonance study of lithium insertion in hard-carbon anode materials for Li-ion batteries," *Journal of Chemical Physics*, vol. 118, no. 13, pp. 6038–6045, 2003.

[14] H. Fujimoto, A. Mabuchi, K. Tokumitsu, N. Chinnasamy, and T. Kasuh, " ^{7}Li nuclear magnetic resonance studies of hard carbon and graphite/hard carbon hybrid anode for Li ion battery," *Journal of Power Sources*, vol. 196, no. 3, pp. 1365–1370, 2011.

[15] Y. Wu, S. Fang, and Y. Jiang, "Carbon anodes for a lithium secondary battery based on polyacrylonitrile," *Journal of Power Sources*, vol. 75, no. 2, pp. 201–206, 1998.

[16] J. Machnikowski, B. Grzyb, J. V. Weber, E. Frackowiak, J. N. Rouzaud, and F. Béguin, "Structural and electrochemical characterisation of nitrogen enriched carbons produced by the co-pyrolysis of coal-tar pitch with polyacrylonitrile," *Electrochimica Acta*, vol. 49, no. 3, pp. 423–432, 2004.

[17] J. Jin, Z. Q. Shi, and C.-Y. Wang, "The structure and electrochemical properties of carbonized polyacrylonitrile microspheres," *Solid State Ionics*, vol. 261, pp. 5–10, 2014.

[18] J. K. Lee, K. W. An, J. B. Ju et al., "Electrochemical properties of PAN-based carbon fibers as anodes for rechargeable lithium ion batteries," *Carbon*, vol. 39, no. 9, pp. 1299–1305, 2001.

[19] C. Kim, K. S. Yang, M. Kojima et al., "Fabrication of electrospinning-derived carbon nanofiber webs for the anode material of lithium-ion secondary batteries," *Advanced Functional Materials*, vol. 16, no. 18, pp. 2393–2397, 2006.

[20] I. Mochida, C.-H. Ku, S.-H. Yoon, and Y. Korai, "Anodic performances of anisotropic carbon derived from isotropic quinoline pitch," *Carbon*, vol. 37, no. 2, pp. 323–327, 1999.

[21] A. Piotrowska, K. Kierzek, P. Rutkowski, and J. Machnikowski, "Properties and lithium insertion behavior of hard carbons produced by pyrolysis of various polymers at 1000 °C," *Journal of Analytical and Applied Pyrolysis*, vol. 102, pp. 1–6, 2013.

[22] D. D. Edie and J. J. McHugh, "High performance carbon fibers," in *Carbon Materials for Advanced Technologies*, pp. 119–138, Pergamon, Amsterdam, The Netherlands, 1999.

[23] I. Isaev, G. Salitra, A. Soffer, Y. S. Cohen, D. Aurbach, and J. Fischer, "A new approach for the preparation of anodes for Li-ion batteries based on activated hard carbon cloth with pore design," *Journal of Power Sources*, vol. 119–121, pp. 28–33, 2003.

[24] Y. Ohzawa, Y. Yamanaka, K. Naga, and T. Nakajima, "Pyrocarbon-coating on powdery hard-carbon using chemical vapor infiltration and its electrochemical characteristics," *Journal of Power Sources*, vol. 146, no. 1-2, pp. 125–128, 2005.

[25] I. A. S. Edwards, "Structure in carbons and carbon forms," in *Introduction to Carbon Science*, H. Marsh, Ed., pp. 1–36, Butterworths, London, UK, 1989.

[26] M. M. Dubinin, "Fundamentals of the theory of adsorption in micropores of carbon adsorbents: characteristics of their adsorption properties and microporous structures," *Carbon*, vol. 27, no. 3, pp. 457–467, 1989.

[27] F. Stoeckli, E. Daguerre, and A. Guillot, "The development of micropore volumes and widths during physical activation of various precursors," *Carbon*, vol. 37, no. 12, pp. 2075–2077, 1999.

[28] A. V. Neimark, Y. Lin, P. I. Ravikovitch, and M. Thommes, "Quenched solid density functional theory and pore size analysis of micro-mesoporous carbons," *Carbon*, vol. 47, no. 7, pp. 1617–1628, 2009.

[29] D. Cazorla-Amorós, J. Alcañiz-Monge, M. A. de la Casa-Lillo, and A. Linares-Solano, "CO_2 as an adsorptive to characterize carbon molecular sieves and activated carbons," *Langmuir*, vol. 14, no. 16, pp. 4589–4596, 1998.